



UWB MIMO antenna with 4-element, compact size, high isolation and single band rejection for high-speed wireless networks

Ahmed A. Ibrahim¹ · Mohamed Fathy Abo Sree²

Accepted: 24 May 2022 / Published online: 28 June 2022
© The Author(s) 2022

Abstract

In this paper, a miniaturized size UWB 4-element MIMO antenna with a band rejection feature is introduced. The four elements have a rectangular radiator with curved edges and a partial ground plane with an etched slot to enlarge the bandwidth of the suggested structure to operate from 3 up to 12 GHz with $S_{11} \leq -10$ dB. The high isolation between elements was achieved by forming the antennas orthogonally without adding decoupling elements to simplify the design. The suggested design has a size of 47×47 mm² placed on low price FR4 substrate. A simple slot is etched into the radiator to achieve the desired band rejection. The simulated and tested outcomes achieved operated band extended from 3 up to 12 GHz with band rejection feature within 3.3 GHz up to 4.3 GHz to eliminate interference with WIMAX applications and high isolation of more than 22 dB between ports. Also, the antenna fulfills peak gain of 3.5 dBi, envelope correlation coefficient (ECC) < 0.005 , diversity gain (DG) 9.98 dB and channel capacity loss (CCL) < 0.4 bit/s/Hz within the operating bands. The outcomes have good consistency which made the suggested antenna to be used in UWB MIMO systems.

Keywords MIMO antenna · High isolation · UWB antenna · Band rejection · High-speed network

1 Introduction

The recent communication systems need a wide bandwidth, and high transmission data rate to improve the quality services of these modern systems. Therefore, the Federal Communications Commission (FCC) specified a frequency band from 3.1 to 10.6 GHz (7.5 GHz) to be utilized in UWB technology [1]. The antenna is an essential component in the UWB technology; so researchers made several attempts to obtain the best design to fulfill the UWB technology demands such as miniaturized size, low price,

wide bandwidth, and omnidirectional patterns with constant gain [2–7].

Because of the multipath problem introduced by the UWB technology, the multi-input-multi-output (MIMO) technology is utilized to solve it. The technology of MIMO is used to enhance the capacity of the system; so the integration between the two technologies is the best choice for improving the performance of the system. The MIMO antenna should have a small size, high isolation between ports, low cost, and many elements that can be used. Achieving high isolation is the main challenge in the MIMO system. Researchers developed several attempts to enhance the isolation of the UWB MIMO antenna. Some of them used decoupling structures such as stubs [8–10] and the others arranged the antenna elements in an orthogonal layout [11–15].

There are two narrowband frequencies allocated for WiMAX technology around 3.6 GHz and WLAN technology around 5.5 GHz could be overlapped with the UWB bands. So, a band rejection mechanism such as resonators added at a specific location in the patch [16], ground [17], and close to the feed line [18] should be utilized to bypass

✉ Ahmed A. Ibrahim
ahmedabdel_monem@mu.edu.eg

Mohamed Fathy Abo Sree
Mohamed.fathy@aast.edu

¹ Communications and Electronics Department, Faculty of Engineering, Minia University, El-Minia, Egypt

² Electronic and Communication Department, Arab Academy for Science, Technology and Maritime Transport, Cairo 11865, Egypt

this problem. UWB MIMO antenna with band rejection mechanisms is proposed in [12, 19–22]. In [12], 4 ports with band rejection mechanism using L-shaped stubs connected to the semielliptical patch radiator to avoid the band within 3–4 GHz (WiMAX) are introduced. A band-stop structure etched within the ground plane of the four elements UWB MIMO antenna to produce single band rejection is investigated in [19]. In [20], two L-shaped slits to introduce band rejection etched in the ground plane of two elements UWB MIMO are proposed. Quad elements with an L-shaped stub to generate band rejection is discussed in [21]. A stub attached to the ground plane of the 4-port UWB MIMO is utilized to create band rejection as displayed in [22].

In this paper, a compact size 4-port UWB MIMO antenna operated at a frequency band from 3 to 12 GHz and with single-band rejection within 3.3 GHz up to 4.3 GHz (WIMAX application) has been suggested. The suggested antenna elements are arranged perpendicularly to save space and increase the isolation between the elements. The four antenna elements have an overall size of $47 \times 47 \text{ mm}^2$. The MIMO diversity performance results have $\text{ECC} < 0.005$, $\text{DG} 9.98 \text{ dB}$, and $\text{CCL} < 0.4 \text{ bit/s/Hz}$ within the operating bands. The suggested antenna is simulated using the CST suite, fabricated, and tested to confirm the simulated results.

2 Proposed single antenna structure

The 2D configuration structure of the UWB single antenna is illustrated in Fig. 1(a). The fabricated photo of the proposed antenna is shown in Fig. 1(b). The antenna is composed of a rectangular radiator with steps and curved edges on the top of the substrate to enhance the operating frequency band. The antenna has a partial ground plane with a length (L_g) of 6 mm and a rectangular slot of $3.5 \text{ mm} \times 3 \text{ mm}$ etched in it to achieve the desired UWB behaviour. A simple meandered slot with a total length of $\lambda_g/4$ as calculated from Eq. (1) is etched in the rectangular radiator to reduce the interference with other devices working with WiMAX technology.

$$L_{total} = \frac{\lambda_g}{4} = \frac{c}{4f_{notch}\sqrt{\epsilon_{eff}}} \tag{1}$$

The low price FR4 substrate with 1.6 mm thick and 4.4 dielectric constant is proposed and utilized in the fabrication process.

Figure 2 illustrates the S_{11} simulated and measured results and the simulated result without using a slot in the radiator. From the simulated results, the antenna without a slot is worked with $S_{11} \leq -10 \text{ dB}$ at frequency band from 3.5 up to 12 GHz. While the antenna with a slot is operated

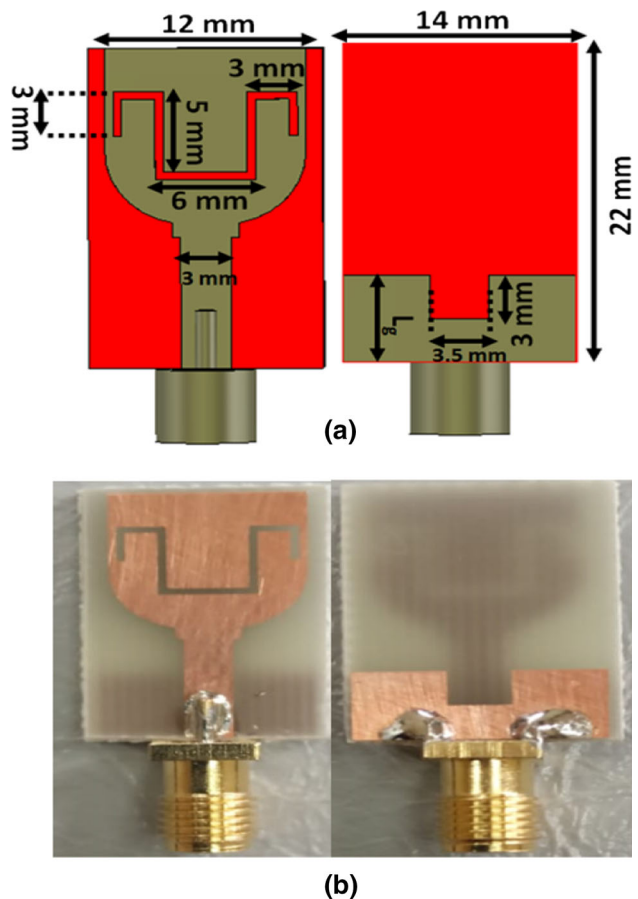


Fig. 1 Proposed single antenna structure **a** 2 D structure **b** Fabricated prototype

from 3 up to 12 GHz with $S_{11} \leq -10 \text{ dB}$ instead of the region from 3.3 to 4.1GHz (the band notched) with a center band of the notch around 3.7 GHz and $S_{11} \geq -10 \text{ dB}$. From the measured results, the antenna is worked at a frequency band with $S_{11} \leq -10 \text{ dB}$ from 3 up to 12 GHz except for the frequency of the band notched from 3.3 to 4.3 GHz with a center band of the notch around 3.7 GHz. The two results have the same trend with a small shift between them because of the fabrication process and human errors due to the soldering.

There are four steps are executed to transfer the proposed antenna from the initial design to the proposed structure as shown in Fig. 3. The first step is the simple rectangular patch with a partial ground plane ($L_g = 6 \text{ mm}$). The antenna is operated with $S_{11} \leq -10 \text{ dB}$ from 3.7 up to 5 GHz as shown in Fig. 3 (the dotted red curve). The second step with the same length as the ground plane and the patch has a step and curved edges. The antenna is worked with two bands from 3.7 to 4.8 GHz and from 7 up to 11 GHz (the dashed blue curve). The third step is the same as the second step except the ground plane has a rectangular slot etched in it. The antenna is operated in

Fig. 2 Simulated and measured S_{11} results of the single antenna structure

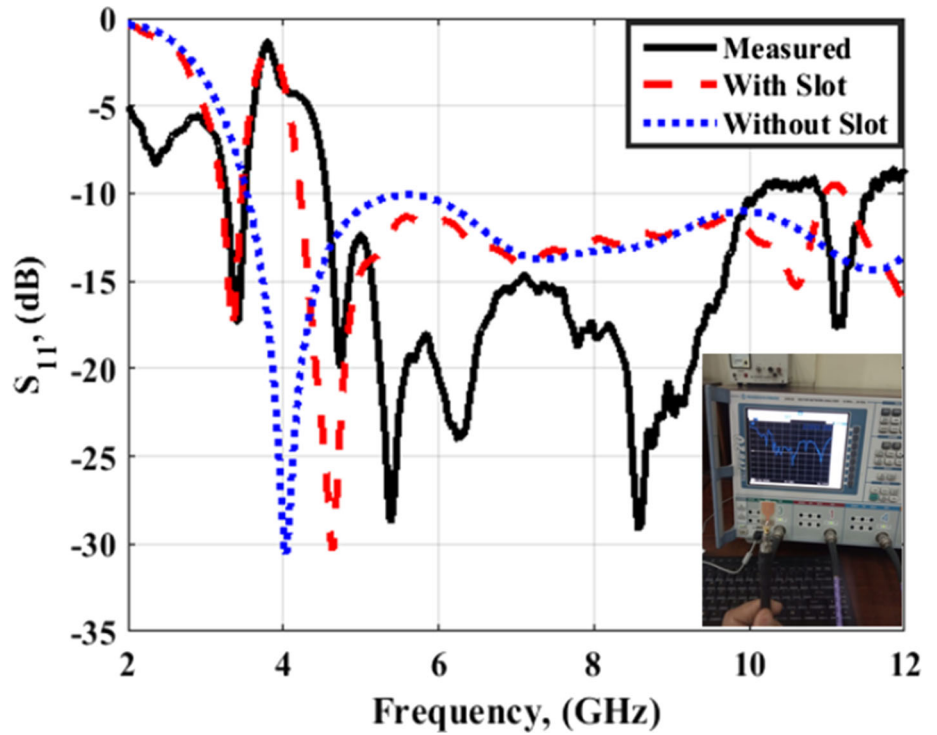
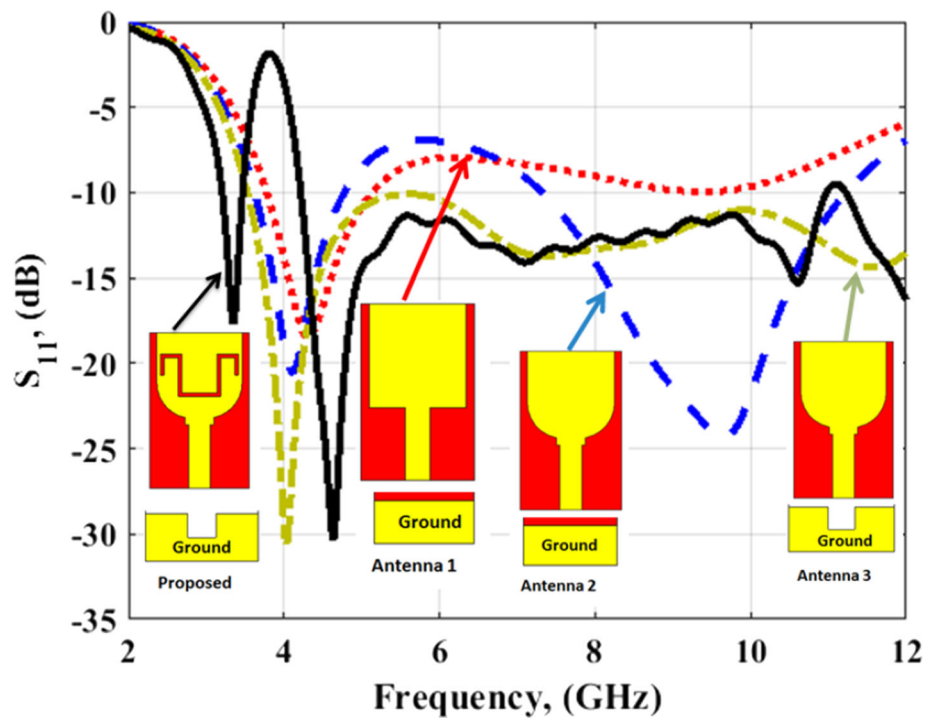


Fig. 3 The simulated S_{11} results and the 2 D configuration of the UWB single antenna structure evolution



UWB operation from 3.5 up to 12 GHz (the dashed green curve). Finally, a simple slot is added to step three to achieve the desired band-notched feature as shown in Fig. 3 (The solid black curve). As well, the ground length (L_g) affects the antenna impedance bandwidth as shown in Fig. 4. The antenna is operated in a narrow band when full

ground with $L_g= 22$ mm is introduced as shown in Fig. 4. By decreasing the ground length, the impedance bandwidth of the antenna is affected as shown in Fig. 4. When $L_g=11$ mm also the narrow band behavior around 14 GHz is presented. When $L_g=6$ mm dual-band operation is introduced. Finally, by etching a simple rectangular slot in the

Fig. 4 Simulated S_{11} results of UWB single antenna structure at different ground lengths (L_g)

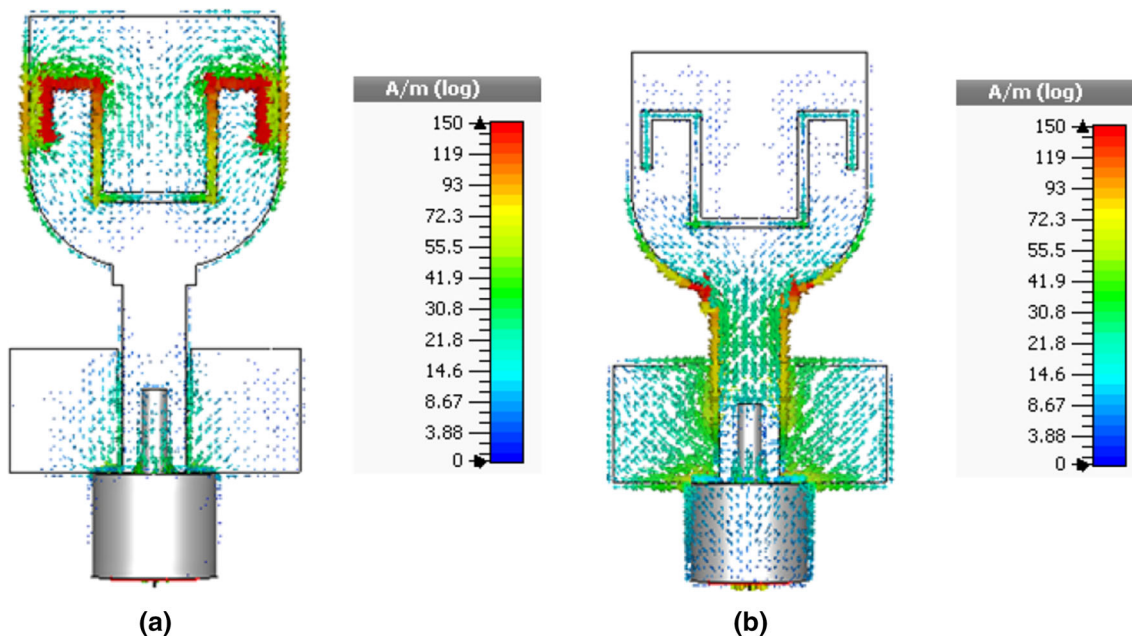
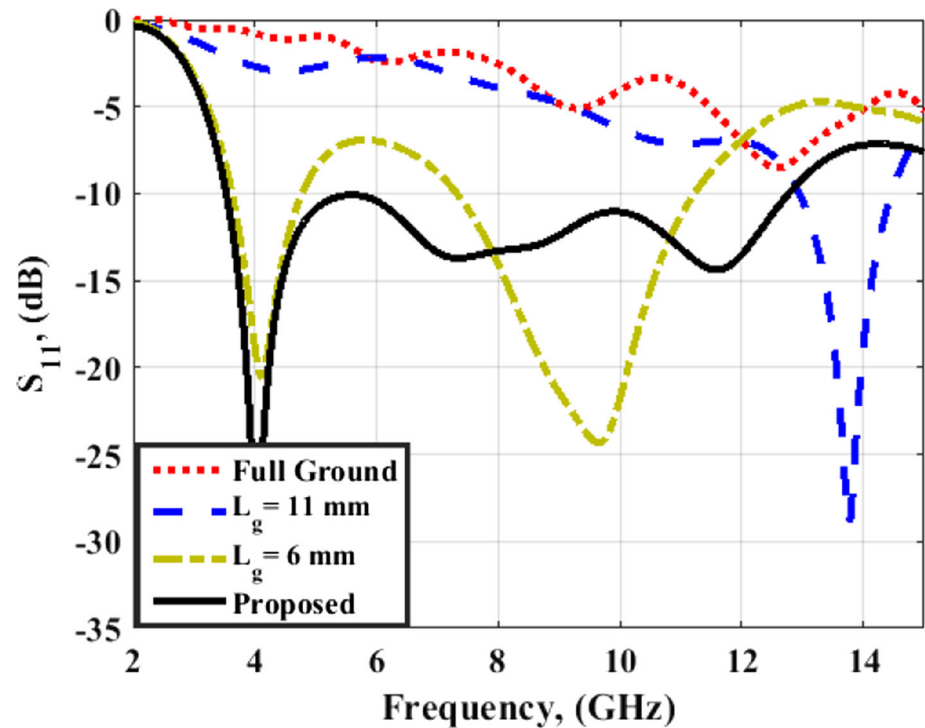


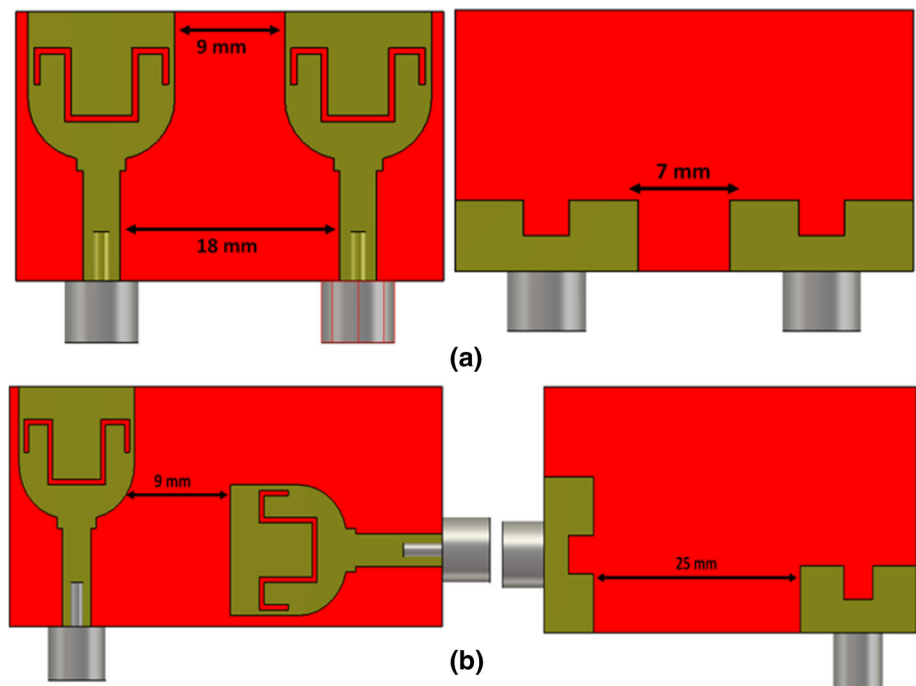
Fig. 5 Simulated current distribution results of UWB single antenna structure **a** @ 3.7 GHz **b** @9 GHz

ground, the UWB feature can be achieved as shown in Fig. 4.

The current distribution simulated results at 3.7 GHz and 8 GHz are illustrated in Fig. 5. The current is collected around the slot in the radiator at the frequency of the notch

as shown in Fig. 5(a) which indicates that the antenna can't radiate at this frequency band. Fig. 5(b) illustrates that the antenna can radiate simply at 8 GHz (frequency away from the notch).

Fig. 6 Two ports UWB antenna layout **a** Side by Side orientation **b** Orthogonal orientation



3 Two-port antenna

The previous single antenna has two orientations to achieve the two ports MIMO operation as shown in Fig. 6. The first one is side by side as shown in Fig. 6(a) and the second is the perpendicular orientation as shown in Fig. 6(b). We don't use any decoupling structure to simplify the antenna structure. The distance between the edges of the two elements is the same as 9 mm ($0.09 \lambda_0$ at 3 GHz) as shown in the figure. The simulated S_{21} is illustrated in Fig. 7. It is noticed that the perpendicular orientation has S_{21} lower than -25 dB within the entire frequency band while the side by side orientation has S_{21} lower than -10 dB, especially at the lower frequency band which means it has high coupling between elements [12–15]. So, the perpendicular orientation is used to form the proposed 4 ports MIMO as discussed in the next section.

4 Four-port proposed antenna

4.1 Layout and S-parameter results

The 2D layout structure of the proposed 4-port antenna is shown in Fig. 8. The antenna has a miniaturized size of $47\text{mm} \times 47\text{mm}$. The antenna elements are arranged based on the previous investigation. The antenna at port 2 has a perpendicular orientation to the antenna at port 1, port 3, and the opposite direction with the same orientation as the antenna at port 4. As well as, the antenna at port 3 has the

same orientation in opposite direction as the antenna at port 1 and perpendicular orientation with the antenna at port 2, port 4. The antenna elements' separation between edges equals 10 mm ($0.1 \lambda_0$ at 3 GHz) as shown in Fig. 8(a). The structure has a symmetry property so; the results from port 1 are extracted only. The MIMO antenna is fabricated and its fabricated prototype photo is illustrated in Fig. 8(b).

The four ports VNA (R&S ZVB 20) is used to test the proposed antenna by gauging the S-parameters to validate the antenna performance. Figure 9 displays the S_{11} simulated and gauged results. It is noticed that the measured result has $S_{11} \leq -10$ at frequency band (UWB) from 3 to 12 GHz except the band notched band from 3.3 to 4.3 GHz. Figure 10 shows the simulated and gauged results of S_{21} , S_{31} , and S_{41} (at port 1). The measured results show that the coupling between antenna elements is lower than -22 dB between antennas (1, 2), antennas (1, 4) (perpendicular orientation), and lower than -18 dB between antennas (1, 3) (same and opposite orientation). This means the proposed antenna has high isolation without using isolation structures. Finally, the gauged and simulated results matched well with small deviation because of fabrication tolerance and process.

Figure 11 shows the simulated current on the surface of the proposed antenna at 3.7 GHz and 9 GHz. As illustrated in Fig. 11(a) the current has a high-level concentration around the slot which enables the antenna to block the radiation at this band. Figure 11(b) displays the distribution of current at 9 GHz. The current has a high-level concentration around the radiator which enables the antenna to

Fig. 7 S_{21} results of the two ports UWB antenna configurations

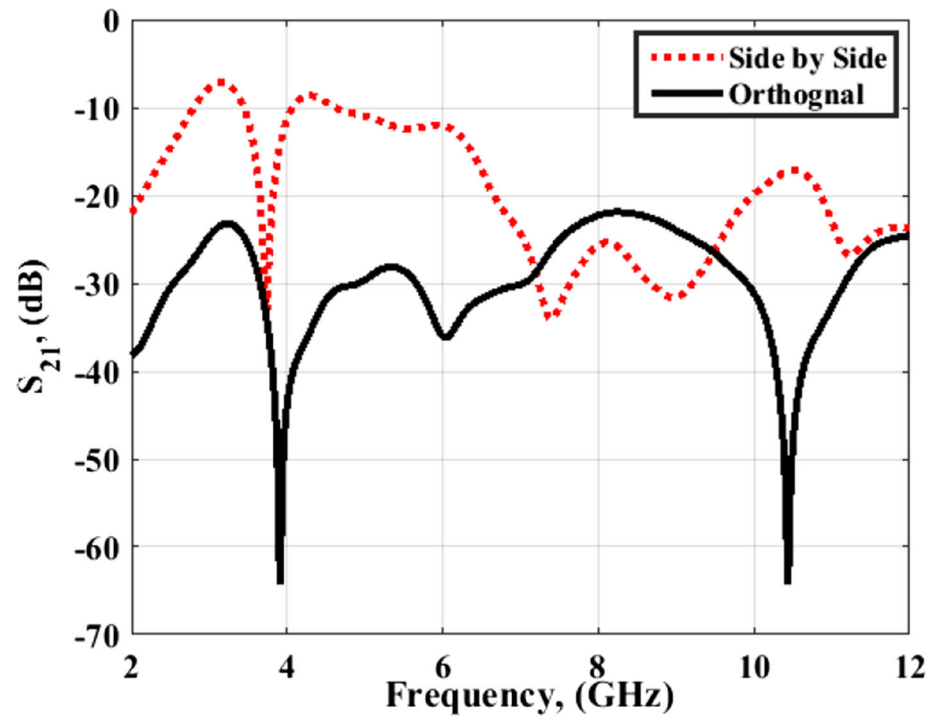


Fig. 8 Layout of the proposed four-port UWB antenna **a** 2 D structure **b** Fabricated prototype

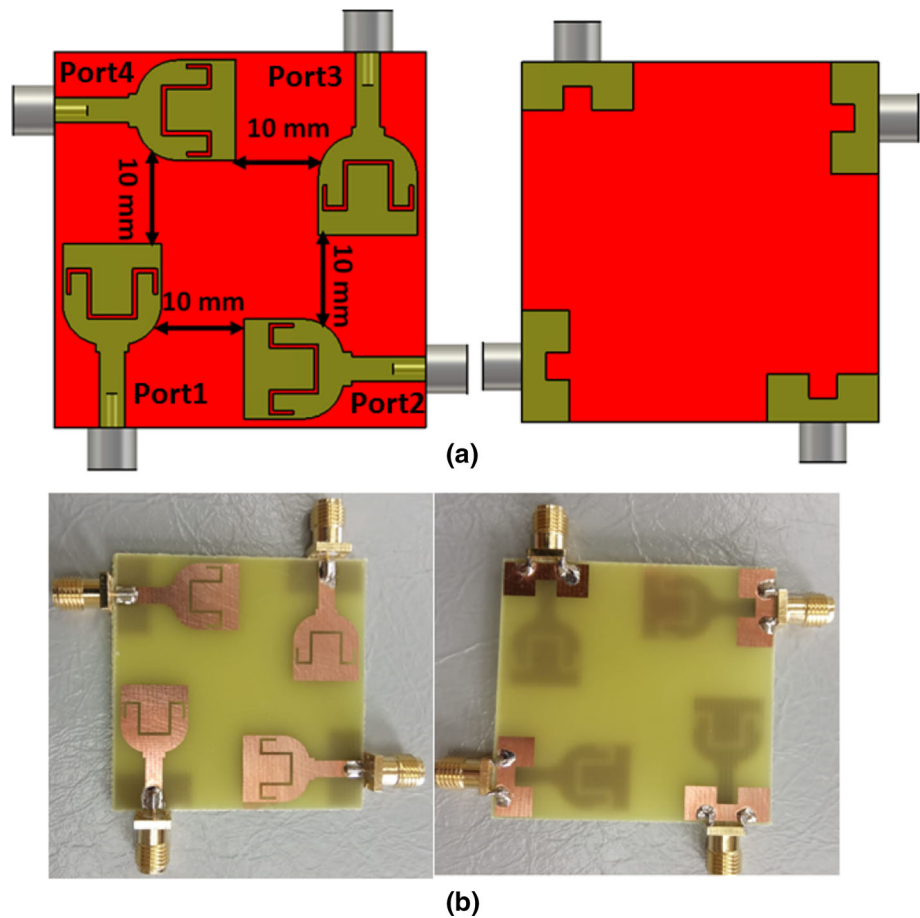


Fig. 9 S_{11} results of the proposed four-port UWB antenna @port 1

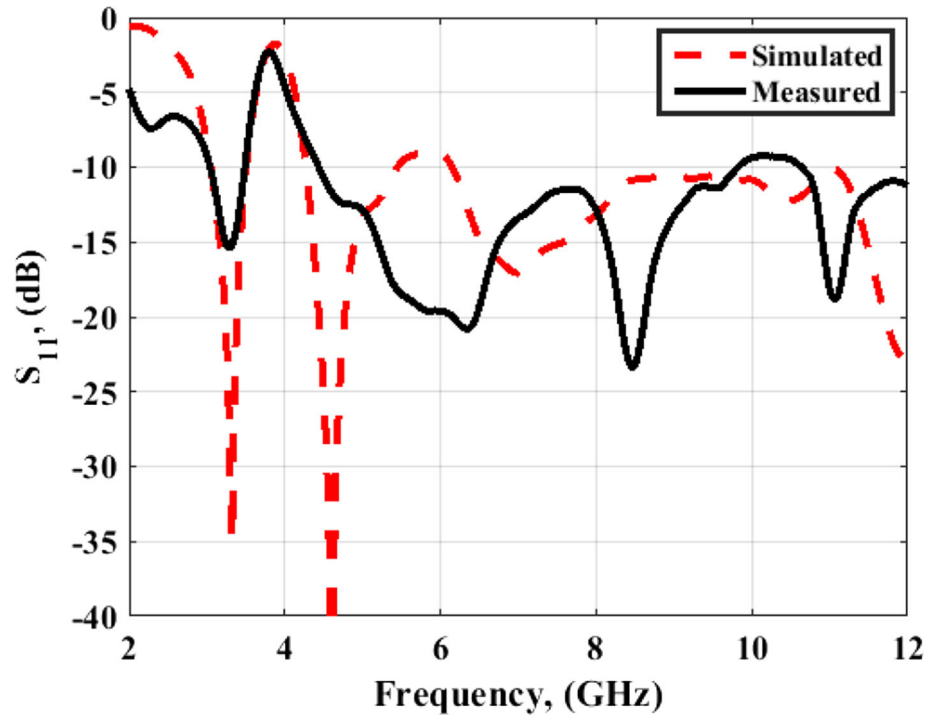
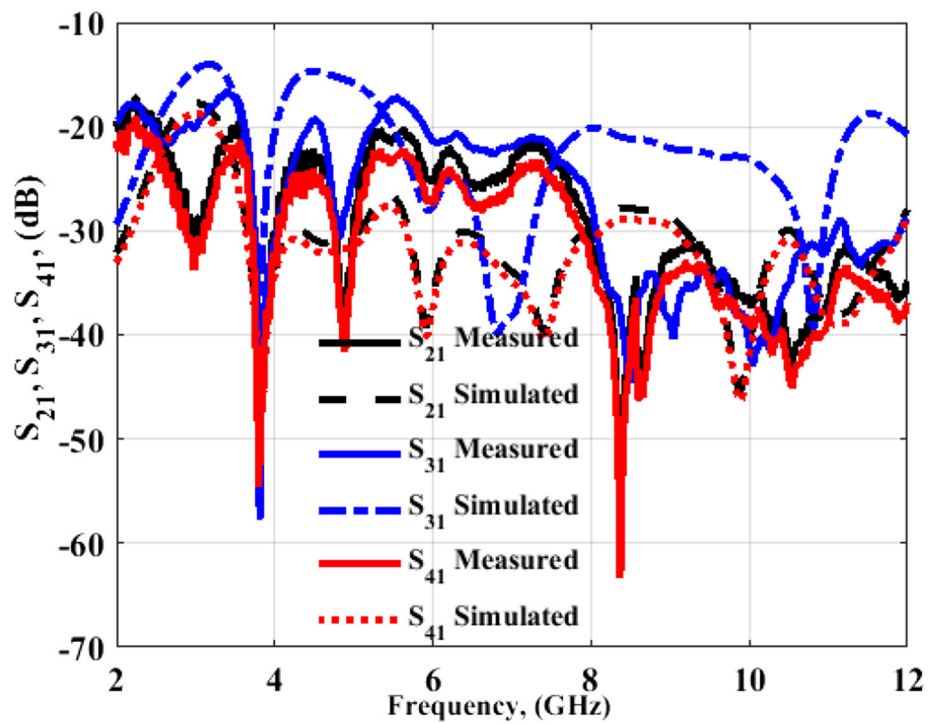


Fig. 10 S_{21} results of the proposed four-port UWB antenna @port 1



radiate at this frequency also there is a small level of current is transmitted to the other three ports which confirms the high isolation between them.

4.2 Radiation patterns

The proposed antenna radiation patterns (at port 1) are measured inside an anechoic chamber and the measuring

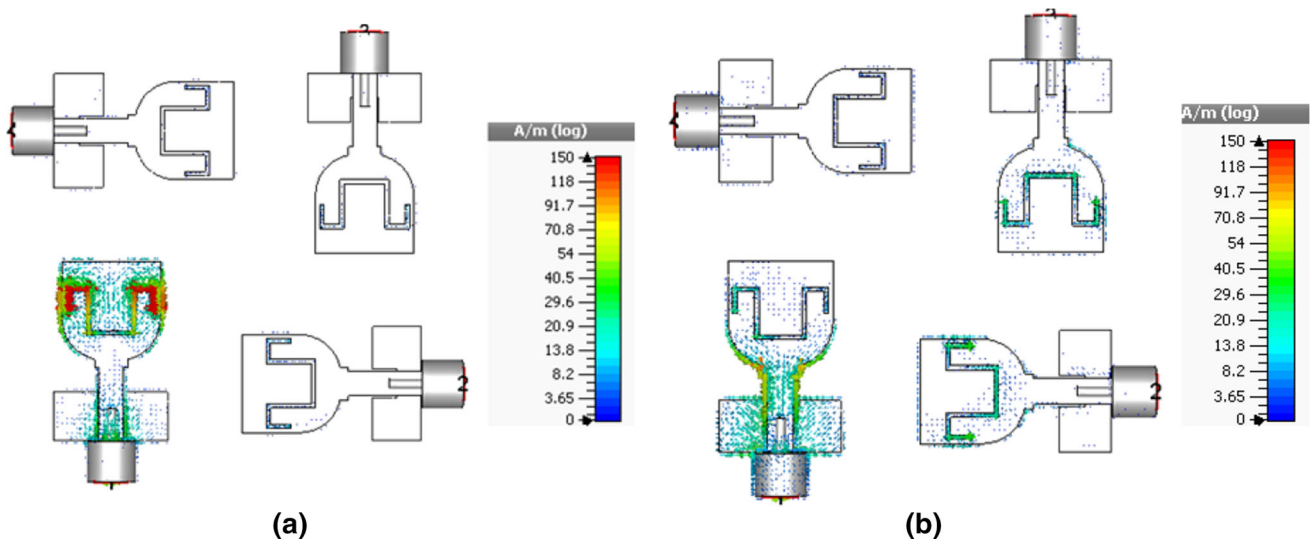
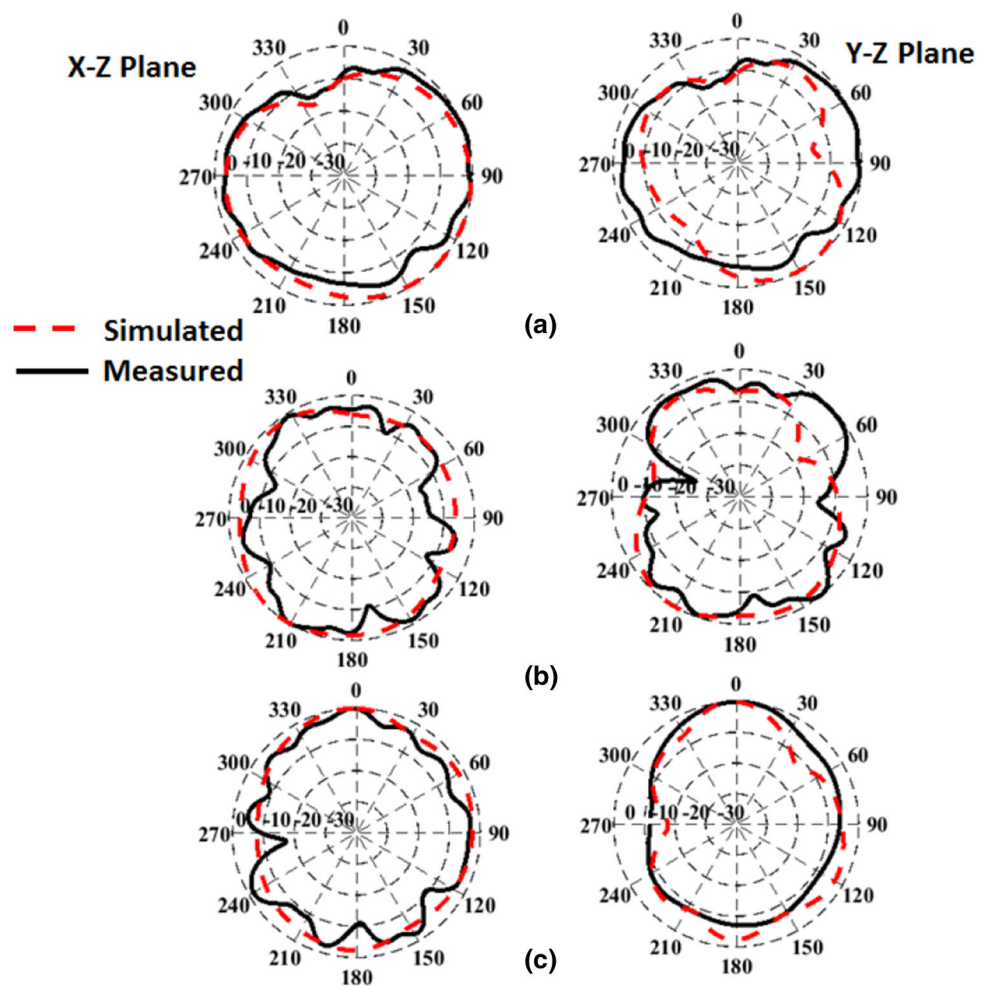


Fig. 11 Current distributions of the proposed four-port UWB antenna @port 1 **a** @ 3.7 GHz **b** @9 GHz

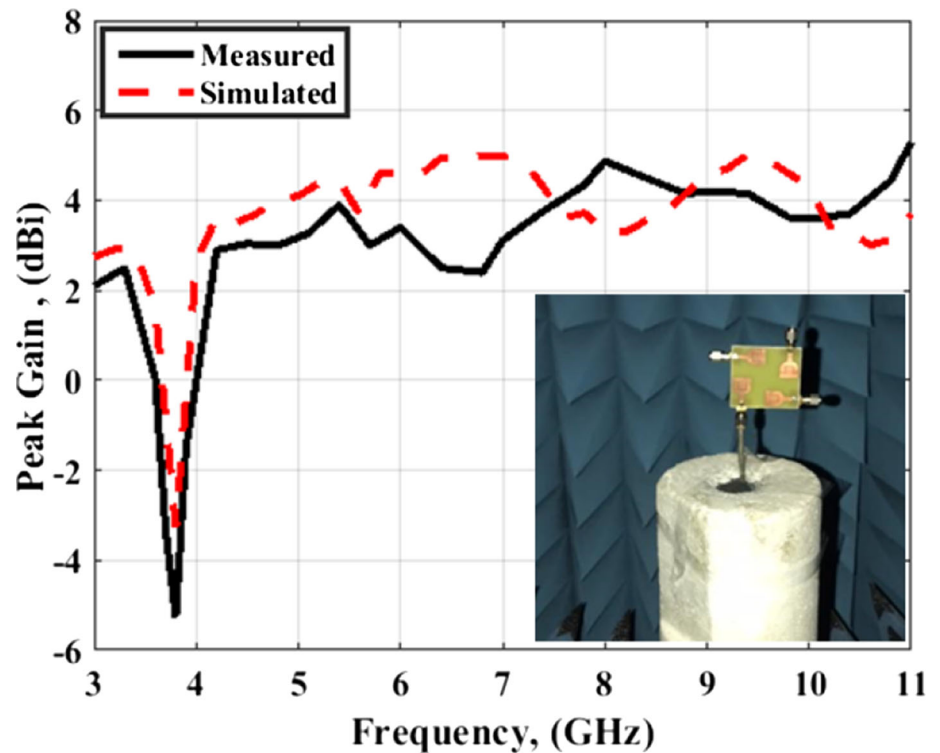
Fig. 12 Normalized radiation pattern results of the proposed four-port UWB antenna @port 1 **a** @ 3.7 GHz **b** @ 7 GHz **c** @ 9.5 GHz



setup is shown in Fig. 13. The radiation patterns in two planes (x-z and y-z) are measured at 3.7 GHz, 7 GHz, and 9.5 GHz, and their normalized results are shown in Fig. 12

when the other three ports are connected with a matched load. As shown, the antenna has semi omnidirectional and semi bidirectional at the x-z plane and y-z plane

Fig. 13 Peak gain results of the proposed four-port UWB antenna @port 1



respectively. Also, the level of the pattern at 3.7 GHz (notched frequency) is low. Finally, the simulated and the measured results have the same tendency to validate the antenna performance. Figure 13 displays the peak gain of the antenna. The antenna has gauged peak gain ranging from 2 to 4 dBi from 3 up to 12 GHz. But the antenna has a peak gain of around - 4 dBi at the frequency band of the notch as shown in Fig. 13.

4.3 4.3 MIMO analysis evaluation

The main three parameters to validate the proposed MIMO performance are ECC, DG, and CCL. The ECC determines the connection between MIMO antenna elements. The ECC with a small value measures the high achievement of the MIMO system. The ECC can be extracted from the far-field results as Eq. (2) [23, 24].

$$ECC = \rho_e = \frac{|\int \int 4\pi [F_1(\theta, \varphi) \cdot F_2(\theta, \varphi) d\Omega]|^2}{\int \int 4\pi |F_1(\theta, \varphi)|^2 d\Omega \int \int 4\pi |F_2(\theta, \varphi)|^2 d\Omega} \quad (2)$$

where, the achieved radiation patterns are $F_i(\theta, \Phi)$.

The ECC simulated and measured results at port (1,2), port (1,3), and port(1,4) are shown in Fig. 14. The measured ECC results have a value lower than 0.005 at all frequency bands except at the notched band equals around 0.01. Also, good matching between the simulated and

measured results has been accomplished. The value of measured ECC is lower than the accepted limit of ≤ 0.5 .

Figure 15 illustrates the measured and simulated DG results which are extracted from Eq. (3) [25].

$$DG = 10 \times \sqrt{1 - |ECC|} \quad (3)$$

The DG has a value higher than 9.98 dB at all frequency bands while equaling 9.96 at the notched band. Finally, the transmission data rates through the channel can be evaluated using CCL (bit/s/Hz). The value of the CCL can be extracted using Eqs. (4), and (5) [26].

$$C(Loss) = -\log_2 \det(\psi^R) \quad (4)$$

$$\psi^R = \begin{bmatrix} \rho_{11} & \rho_{12} \\ \rho_{21} & \rho_{22} \end{bmatrix}, \rho_{ii} = 1 - (|S_{ii}|^2 + |S_{ij}|^2) \quad \text{and} \quad (5)$$

$$\rho_{ij} = -\left(S_{ii}^* S_{ij} + S_{ji}^* S_{ij}\right), \text{for } i, j = 1 \text{ or } 2$$

Figure 16 displays the simulated and gauged results of CCL. The CCL has a value lower than 0.4 bit/s/Hz (the acceptable limits) within the entire frequency band excluding the notched band. In the end, we compare our design with others to validate our novelty. It is clear that our antenna has a compact size with good MIMO performance which promotes our design to be suitable for UWB MIMO systems (Table 1).

Fig. 14 ECC of the proposed four-port UWB antenna @port 1

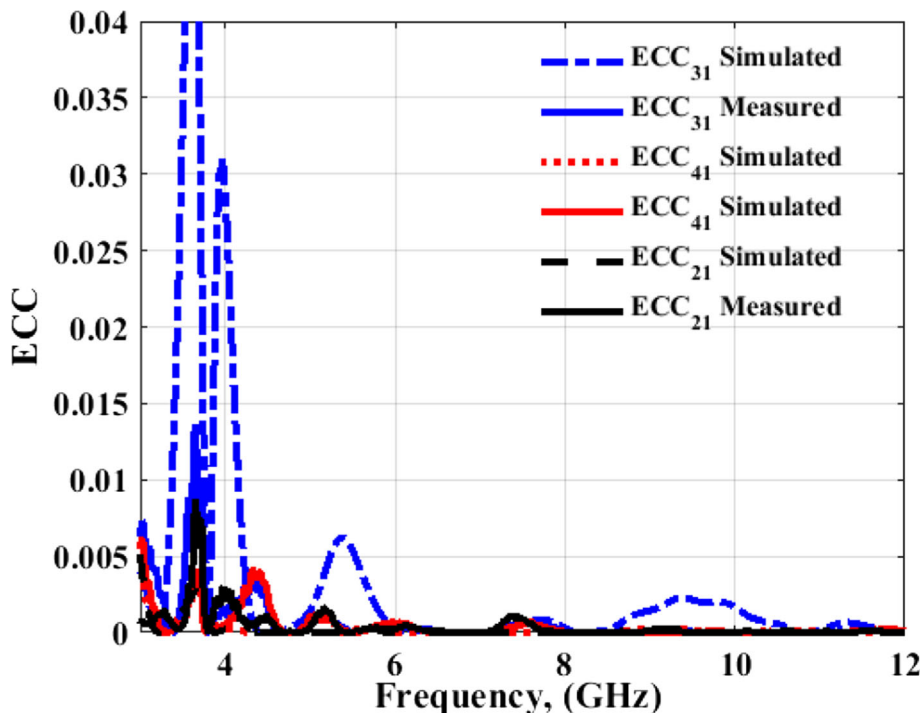
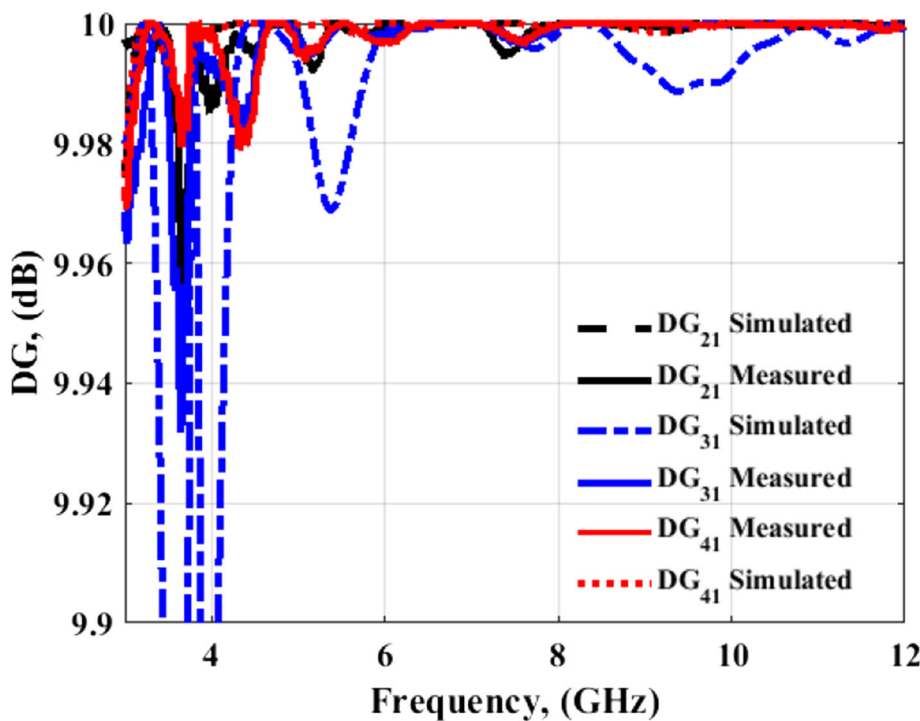


Fig. 15 DG results of the proposed four-port UWB antenna @port 1



5 Conclusion

A small size 4-port UWB MIMO antenna with single-band rejection has been suggested. The simple meandered slot etched in the radiator has been utilized to mitigate the interference with the surrounding WiMAX signal. The suggested MIMO has been placed on $47 \times 47 \times 1.6 \text{ mm}^3$

FR4 substrates. The low mutual coupling between elements has been realized by forming the antennas orthogonally without adding decoupling elements. The antenna has been worked within 3 GHz up to 12 GHz with > 22 dB isolation and band rejection band within 3.3 GHz up to 4.3 GHz. The suggested antenna has omnidirectional radiation patterns with a peak gain of 3.5 dBi except for the band rejection

Fig. 16 CCL results of the proposed four-port UWB antenna @port 1

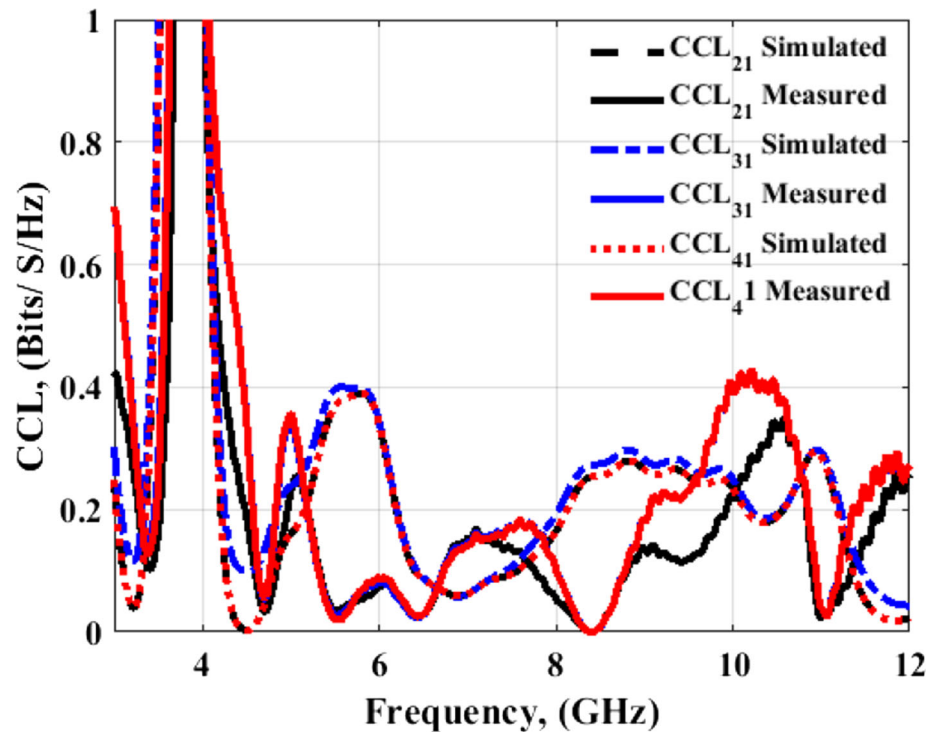


Table 1 Comparison of the suggested design with other previous designs

Refs.	Size mm ²	εr/thickness (mm)	B.W (GHz)	Isolation (dB)	ECC	No. of notches	Ports
[8]	42 × 42	4.4/1.6	3.2–12	> 17	< 0.01	–	4
[12]	48 × 52	4.4/1.6	2.7–11	> 20	< 0.0004	1	4
[14]	81 × 87	4.4/1.6	3.03–10.74	≥ 20	< 0.1	2	4
[19]	50 × 39.8	4.5/1.52	2.7–12	> 17	< 0.01	1	4
[20]	38.5 × 38.5	4.4/1.6	3.08–11.8	> 15	< 0.02	1	2
[21]	44 × 44	4.4/1.6	2.95–10.8	> 15.5	< 0.04	1	4
[22]	50 × 50	4.4/1.6	2–12	> 17	< 0.45	1	4
This work	47 × 47	4.4/1.6	3–12	≥ 22	< 0.005	1	4

bands the peak gain has − 4dBi. The MIMO diversity performance has been discussed and achieved good results with ECC < 0.005, DG 9.98 dB, and CCL < 0.4 bit/s/Hz within the operating bands. The suggested antenna is compared with other previous antennas, and the outcomes illustrate that the suggested antenna is a good choice for band rejection UWB MIMO applications.

Funding Open access funding provided by The Science, Technology & Innovation Funding Authority (STDF) in cooperation with The Egyptian Knowledge Bank (EKB).

Data availability The authors declare that the data supporting the findings of this study are available within the article.

Open Access This article is licensed under a Creative Commons Attribution 4.0 International License, which permits use, sharing, adaptation, distribution and reproduction in any medium or format, as long as you give appropriate credit to the original author(s) and the source, provide a link to the Creative Commons licence, and indicate if changes were made. The images or other third party material in this article are included in the article’s Creative Commons licence, unless indicated otherwise in a credit line to the material. If material is not included in the article’s Creative Commons licence and your intended use is not permitted by statutory regulation or exceeds the permitted use, you will need to obtain permission directly from the copyright holder. To view a copy of this licence, visit <http://creativecommons.org/licenses/by/4.0/>.

References

1. First Report and Order. (2002). Revision of part 15 of the commission's rule regarding ultra-wideband transmission system FCC 02-48, Federal Communications Commission.
2. Lin, C. C., Tang, T. C., Lin, K. H. (2013). Broadband MIMO antennas for MIMO radar systems. In *IEEE Antennas and Propagation Society International Symposium (APSURSI)*, pp. 372–373.
3. Reddy, G. S., Kamma, A., Mishra, S. K., Mukherjee, J. (2014). Compact bluetooth/UWB dual-band planar antenna with quadruple band-notch characteristics. In *IEEE Antennas and Wireless Propagation Letters*, vol. 13, pp. 872–875.
4. Boutejdar, A., Ibrahim, A. A., & Burte, E. P. (2015). Novel microstrip antenna aims at UWB applications. *Microwaves & RF magazine*, 7(7), 8–14.
5. Dhasarathan, V., Sharma, M., Kapil, M., Vashist, P. C., Patel, S. K., & Nguyen, T. K. (2020). Integrated bluetooth/LTE2600 superwideband monopole antenna with triple notched (WiMAX/WLAN/DSS) band characteristics for UWB/X/Ku band wireless network applications. *Wireless Networks*. <https://doi.org/10.1007/s11276-019-02230-0>
6. Deng, J. Y., Guo, L. X., & Liu, X. L. (2015). An ultrawideband MIMO antenna with a high isolation. *IEEE Antennas and Wireless Propagation Letters*, 15, 182–185.
7. Ali, W. A. E., Mohamed, H. A., Ibrahim, A. A., & Hamdalla, M. Z. M. (2019). Gain improvement of tunable band-notched UWB antenna using metamaterial lens for high speed wireless communications. *Microsystem Technologies*, 25(11), 4111–4117.
8. Aboelleil, H., Ibrahim, A. A., & Khalaf, A. A. M. (2021). A compact multiple-input multiple-output antenna with high isolation for wireless applications. *Analog Integrated Circuits and Signal Processing*, 108, 17–24.
9. Khan, M. S., Capobianco, A.-D., Najam, A. I., Shoaib, I., Autizi, E., & Shafique, M. F. (2014). Compact ultra-wideband diversity antenna with a floating parasitic digitated decoupling structure. *IET Microwaves, Antennas & Propagation*, 8, 747–753.
10. Khan, S., Capobianco, A.-D., Iftikhar, A., Shubair, R. M., Anagnostou, D. E., & Braaten, B. D. (2017). Ultra-compact dual-polarised UWB MIMO antenna with meandered feeding lines. *IET Microwaves, Antennas & Propagation*, 11, 997–1002.
11. Sipal, D., Abegaonkar, M. P., & Koul, S. K. (2017). Easily extendable compact planar UWB MIMO antenna array. *IEEE Antennas and Wireless Propagation Letters*, 16, 2328–2331.
12. Ibrahim, A., & Ali, W. (2021). High isolation 4-element ACS-fed MIMO antenna with band notched feature for UWB communications. *International Journal of Microwave and Wireless Technologies*. <https://doi.org/10.1017/S175907872100009X>
13. Khan, M. S., Capobianco, A.-D., Naqvi, A., Ijaz, B., Asif, S., & Braaten, B. D. (2015). Planar, compact ultra-wideband polarisation diversity antenna array. *IET Microwaves, Antennas & Propagation*, 9, 1761–1768.
14. Srivastava, K., Kumar, A., Kanaujia, B. K., Dwari, S., & Kumar, S. (2018). A CPW-fed UWB MIMO antenna with integrated GSM band and dual band notches. *International Journal of RF and Microwave Computer Aided Engineering*. <https://doi.org/10.1002/mmce.21433>
15. Ibrahim, A. A., Machac, J., & Shubair, R. M. (2017). Compact UWB MIMO antenna with pattern diversity and band rejection characteristics. *Microwave and Optical Technology Letters*, 59(6), 1460–1464.
16. Ali, W., Ibrahim, A. A., & Machac, J. (2017). Compact size UWB monopole antenna with triple band-notches. *Radioengineering*, 26(1), 57–63.
17. Mirmosaei, S., Afjei, S., Mehrshahi, E., & Fakharian, M. (2016). A dual band-notched ultra-wideband monopole antenna with spiral-slots and folded SIR-DGS as notch band structures. *International Journal of Microwave and Wireless Technologies*, 8(8), 1197–1206.
18. Salamin, M. A., Ali, W., & Zugari, A. (2019). Design and analysis of a miniaturized band-notched planar antenna incorporating a joint DMS and DGS band-rejection technique for UWB applications. *Microsystem Technologies*, 25, 3375–3385.
19. Khan, M. S., et al. (2015). Compact 4×4 UWB-MIMO antenna with WLAN band rejected operation. *Electronics Letters*, 51, 1048–1050.
20. Kang, L., et al. (2015). Compact offset microstrip-fed MIMO antenna for band-notched UWB applications. *IEEE Antennas and Wireless Propagation Letters*, 14, 1754–1757.
21. Liu, Y. Y., & Tu, Z. H. (2016). Compact differential band-notched stepped-slot UWB-MIMO antenna with common-mode suppression. *IEEE Antennas and Wireless Propagation Letters*, 16, 593–596.
22. Khan, M. S., Naqvi, S. A., Iftikhar, A., Asif, S. M., Fida, A., & Shubair, R. M. (2020). A WLAN band-notched compact four element UWB MIMO antenna. *International Journal of RF and Microwave Computer-Aided Engineering*, 30, e22282.
23. Blanch, S., Romeu, J., & Corbella, I. (2003). Exact representation of antenna system diversity performance from input parameter description. *Electronics Letters*, 39(9), 705.
24. Ibrahim, A. A., & Ali, W. A. E. (2021). High gain, wideband and low mutual coupling AMC-based millimeter wave MIMO antenna for 5G NR networks. *AEU-International Journal of Electronics and Communications*, 142, 153990.
25. Rosengren, K., & Kildal, P. S. (2006). Radiation efficiency, correlation, diversity gain and capacity of a six monopole antenna array for a MIMO system: Theory, simulation and measurement in reverberation chamber. *IEE Proceedings Microwaves, Antennas and Propagation*, 153(6), 400.
26. Shin, H., & Lee, J. H. (2003). Capacity of multiple-antenna fading channels: Spatial fading correlation, double scattering, and keyhole. *IEEE Transactions on Information Theory*, 49, 2636–2647.

Publisher's Note Springer Nature remains neutral with regard to jurisdictional claims in published maps and institutional affiliations.



Ahmed A. Ibrahim (M'19, SM'20). He received the B.Sc. degree, and M.Sc., Ph.D. in Electrical Engineering from the Electronic and Communication Engineering Department, Minia University, El-Mina, Egypt in 2007, 2011, and 2014 respectively. He is now an associated Professor in the electrical engineering department in the faculty of engineering Minia University. He has been a Visiting Professor at University Pierre and Marie Curie, Sorbonne University, Paris VI, France for 7 months and Otto-von-Guericke-Universität Magdeburg-Germany for 6 months. He has published more than 100 peer-reviewed journals and conference papers. His research has focused on miniaturized multiband antennas/wideband, microwave/millimeter components, DRA metamaterial antenna, graphene antenna, and microwave filters. Also, his research

includes MIMO antennas and energy harvesting systems. Dr. Ahmed A Ibrahim is a senior member of the IEEE and a senior member in URSI also a member of the national committee of radio science in Egypt. He is currently a reviewer in, IEEE Antennas and Wireless Propagation Letters, IEEE Microwave Wireless Components, IEEE access, IET Microwave, Antenna and Propagation, IET Electronics Letters, MOTL, Analog Integrated Circuits, and Signal Processing, and many other journals and conferences. In 2020, and 2021 he was named in the top 2% of scientists in “A standardized citation metrics author database annotated for scientific field / ”Updated science-wide author databases of standardized citation indicators“.



Mohamed Fathy Abo Sree was born in Egypt. He received the M.Sc. Degree from the Arab Academy for Science and Technology (AASTMT) in 2013, and the Ph.D. degree in electrical engineering from Ain Shams University, Egypt, in 2019. His research interests include antenna design and MW technology. He made a team of research over 20 members from 7 countries all over the world, he was published 35 papers in different journal and

international conference. He is reviewing in IEEE Access and PIER online Journal.